AJNR

The parenchymal CT myelogram: in vivo imaging of the gray matter of the spinal cord.

J R Jinkins, R Bashir, M Z Al-Kawi and E Siquiera

AJNR Am J Neuroradiol 1987, 8 (6) 979-982
http://www.ajnr.org/content/8/6/979

The Parenchymal CT Myelogram:
In Vivo Imaging of the Gray Matter of the Spinal Cord

John R. Jinkins[1,2]
Rifaat Bashir[3]
M. Zuheir Al-Kawi[3]
Edir Siquiera[4]

Past attempts to visualize the internal structure of the spinal cord in vivo have been hampered by many factors, including the small size of the cord, the dense bony investiture of the spine, and the similarities of tissue densities from one region to another within the cord. Delayed CT is the imaging technique currently being used at our institution as an adjunct to iopamidol myelography to visualize the deep gray matter of the cord. This visualization is achieved by a poorly understood differential gray/white-matter enhancement, possibly due to either a shielding effect of the white matter as it envelops the gray matter, a differential absorption rate between gray and white matter, or a greater rate of reabsorption of contrast by the more highly vascularized gray matter.

This method is not being advocated as a primary diagnostic technique due to the lack of reliability in providing successful results from section to section, from patient to patient, and from one time period of delay to the next. Instead, it is an initial attempt to image the basic, intrinsic structure of the spinal cord in vivo, which may herald a valuable advance in imaging methodology.

CT of cerebral structures has achieved a remarkable level of success, and the images continue to improve progressively in detail and clarity. However, the in vivo radiologic demonstration of substructures of the spinal cord has been less successful. Contrast and spatial resolution limitations have thus far thwarted attempts to visualize such basic structures as the major gray- and white-matter divisions of the cord. Possibly, newer imaging techniques will eventually yield anatomic information, but thus far the results have not been gratifying.

This article discusses the potential of aqueous intrathecal contrast agents, in combination with CT, to reveal the simple gray/white-matter substructure of the spinal cord in normal and diseased states. The normal spinal gray matter is known to have a characteristic variation in size and shape with the spinal cord level [1–3]. Pathologic states alter both the shape and measurements of the cord as well as the configuration of the gray matter itself. Generalized cord atrophy, nonspecific focal insult, syringomyelia, and late ischemic injury all demonstrate characteristic changes, comparing well with known histologic correlates.

Materials and Methods

Thirty-five patients were scanned with CT at varying times from 1–10 hr after conventional complete iopamidol myelography. Five- and 10-mm sections were used depending on the clinical situation and indication. The total intrathecal contrast administration was 3 g I in every subject (10 ml of 300 mg/ml I iopamidol). CT filming was done at broad and narrow window widths to illustrate both normal and pathologic conditions of the spinal cord. No adverse reaction due to the administered intrathecal contrast agent was encountered in any of the patients.

Received July 18, 1986; accepted after revision November 25, 1986.

Presented at the XII Symposium Neuroradiologicum, Stockholm, June 1986.

[1] Section of Neuroradiology, King Faisal Specialist Hospital and Research Centre, Riyadh 11211, Saudi Arabia.

[2] Present address: Huntington Medical Research Institutes, NMR Imaging Laboratory, 10 Pico St., Pasadena, CA 91105-3201. Address reprint requests to J. R. Jinkins.

[3] Section of Neurology, King Faisal Specialist Hospital and Research Centre, Riyadh 11211, Saudi Arabia.

[4] Department of Neurosurgery, King Faisal Specialist Hospital and Research Centre, Riyadh 11211, Saudi Arabia.

***AJNR* 8:979–982, November/December 1987**
0195–6108/87/0806–0979

Results

This retrospective study yielded successful images of the deep gray matter in approximately 10% of the total sections obtained. Factors that correlated with visualization included an optimum delay of between 6–8 hr and a 5-mm rather than 10-mm section thickness. A factor that led to a failure of gray-matter visualization was any image degradation, however subtle, including minor patient motion or sectioning through areas commonly fraught with artifact, such as the cervicothoracic junction.

This technique allows the anatomic mapping of the configuration of the gray matter and the correlation of this information with the vertebral segment level. This explicit clinicoanatomic relationship is too often overlooked. The changing morphology of the gray matter at different segmental levels is quite graphically illustrated in various patients (Figs. 1–3).

Additionally, in certain instances, valid observations can be made in various pathologic conditions of the spinal cord. Changes in the configuration of the gray matter are apparent in generalized cord atrophy (Fig. 4), focal idiopathic cord insult (Fig. 5), and syrinx formation (Fig. 6). Remarkably, clinically suspected subacute cord infarction in one patient with transverse myelopathy revealed a reversal in the usual picture, with contrast preferentially collecting in the apparently necrotic deep gray matter (Fig. 7).

Discussion

Aqueous intrathecal contrast penetrance of the CNS has been pointed out and analyzed by many authors [4–24]. Most of the work has been done on the brain. However, how the spinal cord appears with, and is affected by, these contrast agents is not clear.

The correlation of spinal cord anatomy and the physiologic disappearance of substances from the subarachnoid space into the cord substance is being continually clarified [14, 15,

Fig. 1.—Parenchymal CT myelogram at C3 vertebral segment illustrates plump configuration of gray matter excellently outlining the anterior and posterior horns. (8 hr delay; L = 110, W = 20.)

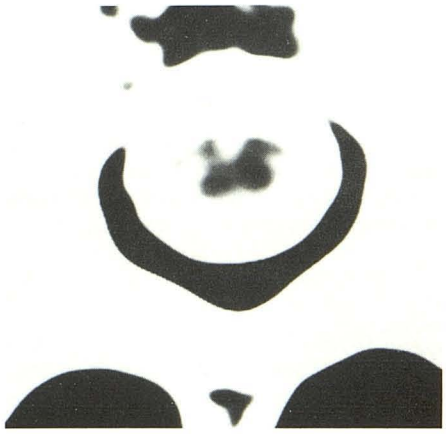

Fig. 2.—Parenchymal CT myelogram at T10 vertebral segment (L1 spinal cord level), shows normal configuration of thoracic cord gray matter at this level. (7 hr delay; L = 140, W = 35.)

Fig. 3.—Parenchymal CT myelogram at T12 vertebral segment (S1 spinal cord level), demonstrates large proportion of gray to white matter at this level in normal subjects. (6 hr delay; L = 100, W = 30.)

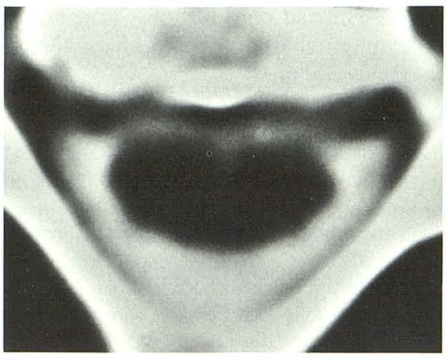

A

B

Fig. 4.—38-year-old man with craniocervical Arnold-Chiari malformation.

***A*, Wide window image at C4 vertebral level demonstrates mildly atrophic cord. (L = 220, W = 300.)**

***B*, Parenchymal CT myelogram at 8 hr illustrates a "consolidated" appearance of deep gray matter with little accompanying surrounding white matter. This indicates marked white-matter (tract) atrophy as compared with relatively normal volume of gray matter at this level. (L = 90, W = 40.)**

Fig. 5.—21-year-old man with Behcet's disease, generalized long-tract signs, and prominently decreased sensation on left side of trunk caudally. Parenchymal CT myelogram at 6 hr depicts truncation of posterior horn on left (*arrow*) correlating with the degree of severity of clinical symptoms corresponding to this level. (L = 160, W = 20.)

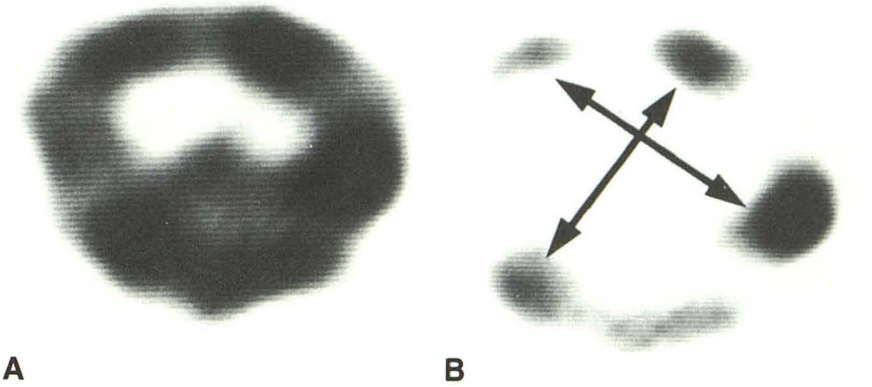

Fig. 6.—25-year-old man with subacute onset of paraparesis, associated rapid progression, and clinical craniad extension.

A, Delayed image at 10 hr after myelogram at T10 vertebral level illustrates syrinx formation centrally. (L = 110, W = 50.)

B, Narrow window technique demonstrates central derangement of deep gray matter, the four horns being displaced outwardly by expanded syrinx cavity (*arrows*). (L = 80, W = 20.)

Fig. 7.—25-year-old man with progressive subacute (4 weeks) transverse myelopathy.

A, Immediate postmyelographic CT shows normal-size cord at T11 vertebral segment, but a somewhat irregular cord surface. (L = 200, W = 100.)

B, Parenchymal CT myelogram after 8-hr delay illustrates complete reversal in typical appearance, with deep gray matter preferentially concentrating contrast material. This suggests an evolving insult, such as infarction, accounting for the progressive myelopathy, with contrast material collecting in the necrotic deep gray matter. (L = 140, W = 30.)

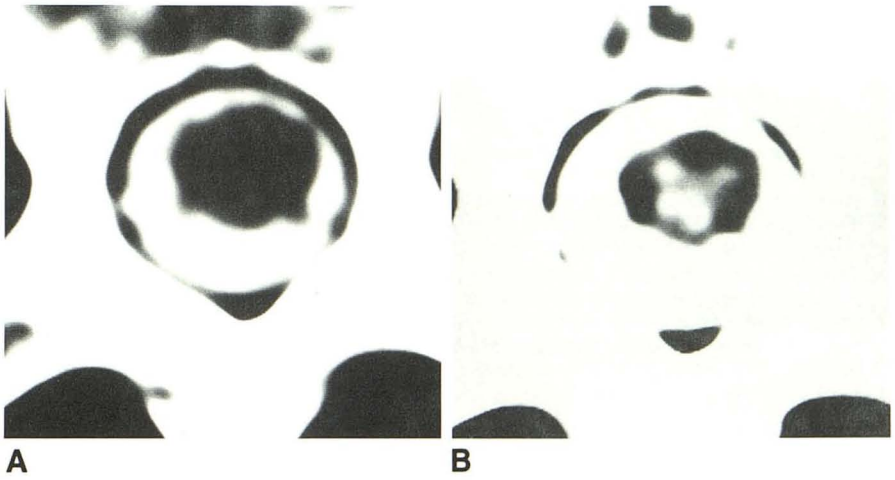

25–31]. That the intrathecally enhanced differentiation of gray from white matter might occur should not be surprising. In the brain the white matter is deep to gray matter, but in the cord the gray matter is in the reverse position; it is "covered" by white matter. Quite possibly, therefore, the means of physiologic penetration and the end result is at least modified, if not totally different. The opposite structural orientation and enhancement pattern of the gray-white matter in the spinal cord as compared with the brain is illustrated by the intense cerebral cortical gray matter enhancement after water-soluble myelography with less relative enhancement of the deep white matter.

The images obtained in this study of the spine, on the other hand, demonstrate that the iopamidol penetrates and opacifies the overlying white matter, while the normal gray matter stands out in negative relief. The possible reasons for this differential contrast uptake are severalfold: (1) the previously mentioned anatomic condition of white matter virtually enveloping the gray matter and thus receiving more contact with higher concentrations of contrast material; (2) microstructural differences in spatial orientation of the gray matter, which is reticulate in its geometric design vs the white matter, which is formed of densely packed parallel tracts; (3) the higher degree of vascularization of the gray matter allowing for more rapid clearance of the contrast agent; and (4) a basic difference in the physiologic interaction of gray and white matter of the spinal cord with nonionic contrast materials.

From this initial attempt to image the substructure of the spinal cord, several conclusions can be drawn: (1) the deep gray matter of the cord can be imaged in normal and pathologic states; (2) the spatial resolution of advanced CT imaging instruments is adequate; (3) contrast resolution is only pos-

sible at present with contrast resolution amplification by means of intrathecal aqueous contrast medium enhancement and delayed imaging; and (4) the ratio of gray matter images obtained to CT sections performed is currently low (≈10%).

ACKNOWLEDGMENTS

We thank Mrs. A. Radford for manuscript preparation, Mrs. C. Jinkins for manuscript research, and the Radiology Department of the King Faisel Specialist Hospital for technical assistance with the illustrations.

REFERENCES

1. Kelly JP. Anatomical basis of sensory perception and motor co-ordination. In: Kandel ER, Schwartz JH, eds. *Principles of neural science*, 2nd ed. New York: Elsevier, **1985**:223–243
2. Martinez Martinez PFA. *Neuroanatomy. Development and structure of the central nervous system*. Philadelphia: Saunders, **1982**:87–92
3. Truex RC, Carpenter MB. *Neuroanatomy*. Baltimore: Williams & Wilkins, **1969**:236–253
4. Cserr HF. Relationship between cerebrospinal fluid and interstitial fluid of brain. *Fed Proc* **1974**;33:2075–2078
5. Caille JM, Guibert-Tranier F, Howa JM, Billerey J, Calabet A, Piton J. Cerebral penetration following metrizamide myelography. *J Neuroradiol* **1980**;7:3–12
6. Cala LA. Cerebral absorption of metrizamide. *Lancet* **1981**;2:922–923
7. Drayer BP, Rosenbaum AE. Metrizamide brain penetrance. *Acta Radiol [Suppl] (Stockh)* **1977**;355:280–293
8. Eldevik OP, Haughton VM, Sasse EA. Elimination of aqueous myelographic contrast media from the subarachnoid space. *Invest Radiol* **1980**;15:S260–S263
9. Fenstermacher JD, Bradbury MWB, du Boulay G, Kendall BE, Radu EW. The distribution of 1251-metrizamide and 1251-diatrizoate between blood, brain and cerebrospinal fluid in the rabbit. *Neuroradiology* **1980**;19:171–180
10. Goldman K. Distribution and retention of 1251-labelled metrizamide after intravenous and suboccipital injection in rabbit, rat and cat. *Acta Radiol [Suppl] (Stockh)* **1973**;355:300–311
11. Golman K, Wiik I, Salvesen S. Absorption of a non-ionic contrast agent from cerebrospinal fluid to blood. *Neuroradiology* **1979**;18:227–233
12. Golman K. Absorption of metrizamide from cerebrospinal fluid to blood: pharmacokinetics in humans. *J Pharm Sci* **1975**;64(3):405–407
13. Hayman LA, Pagani JJ, Anderson GM, Dubravsky N, Bigelow RH. Concentration of intrathecal ^{3}H-labeled metrizamide in normal dog brain: age-related differences. *AJNR* **1983**;4:1091–1096
14. Klatzo I, Miquel J, Ferris PJ, Prokop JD, Smith DE. Observations on the passage of the fluorescein labelled serum proteins (FLSP) from the cerebrospinal fluid. *J Neuropathol Exp Neurol* **1964**;23:18–35
15. Lee JC, Olszewski J. Penetration of radioactive bovine albumin from cerebrospinal fluid into brain tissue. *Neurology* **1960**;10:814–822
16. Levin E, Sisson WB. The penetration of radiolabeled substances into rabbit brain from subarachnoid space. *Brain Res* **1972**;41:145–153
17. Olsson B, Eldevik OP, Gronnerod TA. Absorption of iohexol from cerebrospinal fluid to blood: pharmacokinetics in humans. *Neuroradiology* **1985**;27:172–175
18. Reed DJ, Woodbury DM. Kinetics of movements of iodine, sucrose, inulin and radio-iodinated serum albumin in the central nervous system and cerebrospinal fluid of the rat. *J Physiol (Lond)* **1963**;169:816–850
19. Sage MR, Wilcox J, Evill CA, Benness GT. Brain parenchyma penetration by intrathecal ionic and nonionic contrast media. *AJNR* **1982**;3:481
20. Sage MR, Wilcox J. Brain parenchyma penetration by intrathecal nonionic iopamidol. *AJNR* **1983**;4:1181–1183
21. Sage MR. Kinetics of water-soluble contrast media in the central nervous system. *AJNR* **1983**;4:897–906
22. Speck U, Schmidt R, Volkhardt V, Vogelsang H. The effect of position of patient on the passage of metrizamide (amipaque), meglumine iocarmate (dimer x) and ioserinate (myelografin) into the blood after lumbar myelography. *Neuroradiology* **1978**;14:251–256
23. Vincent FM. CT after metrizamide myelography. *Neurology* **1982**;32:685
24. Winkler SS, Sackett JF. Explanation of metrizamide brain penetration: a review. *J Comput Assist Tomogr* **1980**;4(2):191–193
25. Dubois PJ, Drayer BP, Sage M, Osborne D, Heinz ER. Intramedullary penetrance of metrizamide in the dog spinal cord. *AJNR* **1981**;2:313–317
26. Bonafe A, Manelfe C, Espagno J, Guiraud B, Rascol A. Evaluation of syringomyelia with metrizamide computed tomographic myelography. *J Comput Assist Tomogr* **1980**;4(6):797–802
27. Iwasaki Y, Abe H, Isu T, Miyasaka K. CT myelography with intramedullary enhancement in cervical spondylosis. *J Neurosurg* **1985**;63:363–366
28. Kan S, Fox AJ, Viñuela F, Barnett HJM, Peerless SJ. Delayed CT metrizamide enhancement of syringomyelia secondary to tumor. *AJNR* **1983**;4:73–78
29. Pullicino P, Kendall BE. Computed tomography of "cystic" intramedullary lesions. *Neuroradiology* **1982**;23:117–121
30. Quencer RM, Green BA, Eismont FJ. Posttraumatic spinal cord cysts: clinical features and characterization with metrizamide computed tomography. *Radiology* **1983**;146:415–423
31. Sotaniema KA, Pyhtinen J, Myllyla VV. Computed tomography in the diagnosis of syringomyelia. *Acta Neurol Scand* **1983**;68:121–127